

Supporting Information for ”Pair Selection Optimization for InSAR Time Series Processing”

D. Smittarello¹, N. d'Oreye^{1,2}, M. Jaspard¹, D. Derauw^{1,3,4}, S. Samsonov⁵

¹European Center for Geodynamics and Seismology, 19 rue Josy Welter, L-7256 Walferdange, Gd Duchy of Luxembourg

²National Museum of Natural History, Department of Geophysics/Astrophysics, Rue Josy Welter 19, L-7256 Walferdange,
Grand-Duchy of Luxembourg

³Laboratorio de Estudio y Seguimiento de Volcanes Activos (LESVA), IIPG-Universidad Nacional de Rio Negro - CONICET, 1242
Av. General Roca, 8332, General Roca, Argentina

⁴Centre Spatial de Liège (CSL), Avenue du Pré Aily, B-4031 Angleur, Belgium

⁵Canada Center for Mapping and Earth Observation, Natural Resources Canada (NRCAN), 560 Rochester Street, Ottawa, ON
K1A 0E4, Canada

Contents of this file

1. Text S1 to S2
2. Figures S1 to S21

Introduction The supporting information presented in the following consist in a short text on the baseline criteria selection, on the possible optimization strategies, and a set of figures that illustrate how the coherence behave and how the coherence proxy defined in the main text is calibrated and adjusted to the different data sets used in the study (3 regions, 3 satellites and several acquisition modes).

Text S1. Baseline Criteria Selection The choice of B_T and B_P is critical and depends on the goal of the study. Their choice depends on several criteria that the user must carefully assess and adapt in function of e.g:

- The studied target (e.g. the possible DEM inaccuracies, the type of ground cover, the seasonal decorrelation, the type of expected deformation etc... , which are among the main drivers in the selection of B_T and B_P),
- The satellite (some satellites, such as CSK, have large orbital tubes, which do not favor short baselines between images close in time and hence force the usage of either long B_T or large B_P , or both)
- The computing resources available (the larger the maximum B_T and B_P , the larger the total number of compatible pairs to process, and hence the more space it takes on hard drive and the more it mobilizes the CPU's)
- The time of the processing (the larger the maximum B_T and B_P , the larger the total number of compatible pairs to process, and hence the longer time it takes)
- The type of application (systematic unsupervised processing for automatic monitoring or detailed study of a specific case)
- The speed of expected deformation (fast deformation requires short temporal baselines for avoiding aliasing or decorrelation due to ground cover reshaping, slow deformation requires long temporal baselines to maximize the signal to noise ratio)
- Other types of potential errors such as the fading signal (Ansari et al., 2020).

It is hence the responsibility of the user to find the appropriate values of B_T and B_P given its needs and taking into account these criteria while maintaining a gap-less Baselines Plot (interferometric graph connectivity).

Text S2. Optimization strategies

When the optimization is used in an incremental procedure (i.e. to be run each time a new image is made available), two strategies are possible. The strategies are described here for usage with MasTer, but it could be adapted for usage with other mass processing tools.

When a new image is made available, an original graph is computed (that is the graph of all pairs satisfying the B_T and B_P criteria). MasTer then lists among that graph all the pairs that do not exist in the database yet, that the pairs involving the new image. Here two possibilities exist:

- 1) MasTer computes the deformation maps for all these new compatible pairs so that they all exist in the data base whatever the optimization will select. Optimization then selects among that original graph a subset of pairs, and only these new deformation maps are added to the data base used to perform the MSBAS inversion. This speeds up the inversion process and reduces the noise as we demonstrated. However, it does not reduce the number of deformation maps to compute (because they are all computed), which is the most time-consuming tasks. However, experience shows that each new image requires about the same number of new pairs satisfying B_T and B_P criteria to be processed (as long as the orbital characteristics of the satellite does change). Hence, one knows in average the computer load and processing time a new image will require to update the time series. If that amount of processing load is manageable by the computer infrastructure, it is a convenient strategy as the user is ensured to have all the pairs processed that may be needed.

2) The other possibility consists in only computing the deformation maps for the pairs identified in the optimized graph, not in the original graph. This obviously reduces a lot the number of interferometric pairs to process, which is the most time consuming task. This is hence very convenient in the case of a one-shot study, e.g. a new study on a target area where a large number of images exists but no pairs were processed yet, and no update must be processed as soon as a new image will be made available. However, for the operation of an incremental monitoring ingesting every new image automatically, we can't exclude that a new image wouldn't suddenly destabilize the optimized graph. In such a case, the optimization would select a significantly different path through the original graph, which would in turn require the computation of a very large number of new interferometric pairs (including between old archives). In such a case, the time to process all the missing pairs may exceed by far the time usually required to compute only the small number of pairs involving only the new image, as in the case 1. In the worst case scenario, that processing time might exceed the time up to the delivery of the next image, which might hamper the use of that tool for monitoring purposes. This risk might be more important for instance when monitoring a highly coherent zone using large temporal baseline. For that reason, this second strategy is not recommended for automatic monitoring.

References

- Ansari, H., De Zan, F., & Parizzi, A. (2020). Study of systematic bias in measuring surface deformation with sar interferometry. *IEEE Transactions on Geoscience and Remote Sensing*, 59(2), 1285–1301.

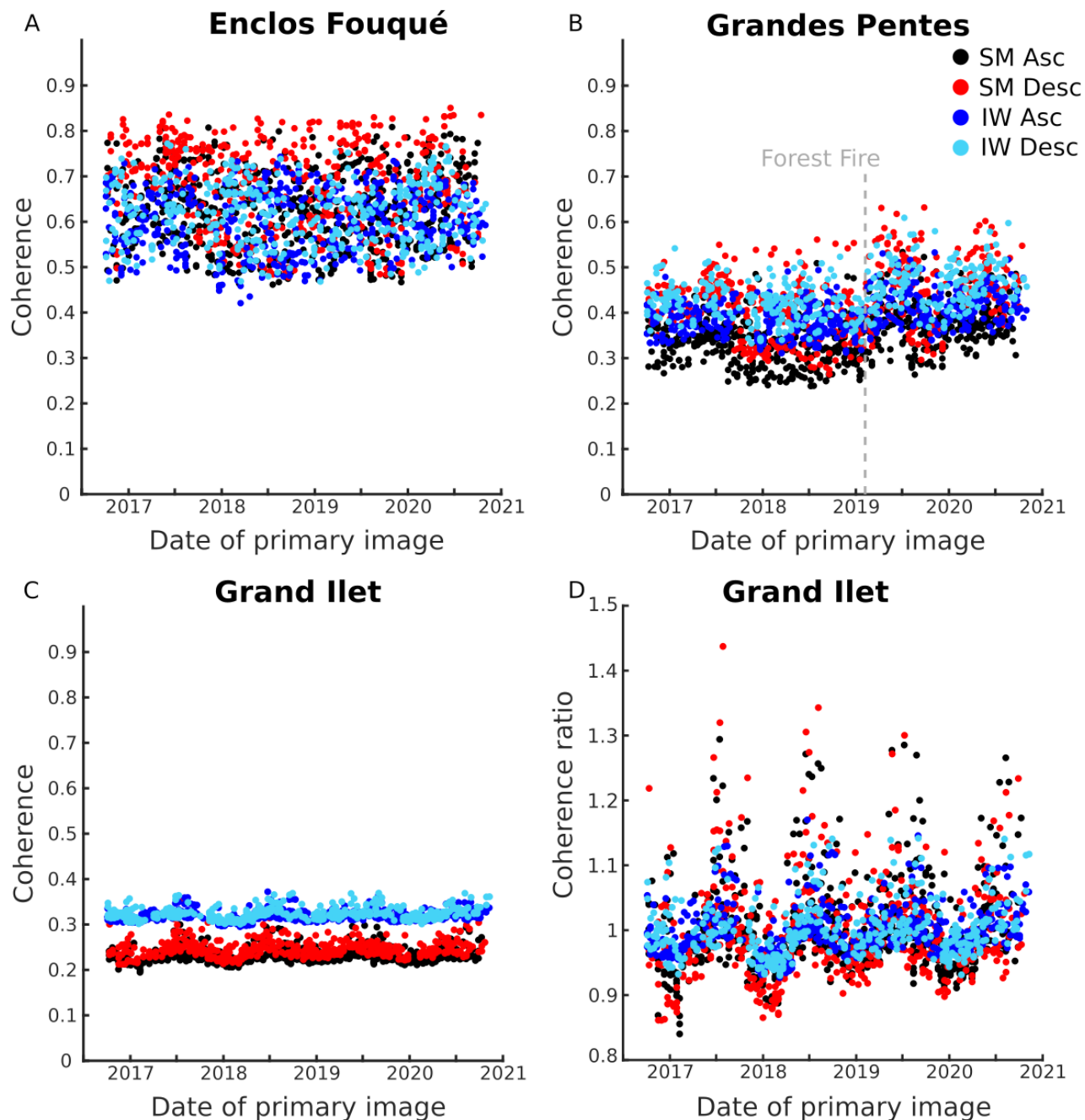


Figure S1. Characteristics of the coherence of the Reunion Island. Each dot represents the mean coherence for each pair of images computed on a ROI defined by a kml files framing the Enclos Fouqué (A), the lower eastern flank (Grandes Pentès (B)) and Grand Ilet (C). On panel D, each dot represents the ratio of the coherence for each pair to the mean value computed from all pairs on the Grand Ilet area.

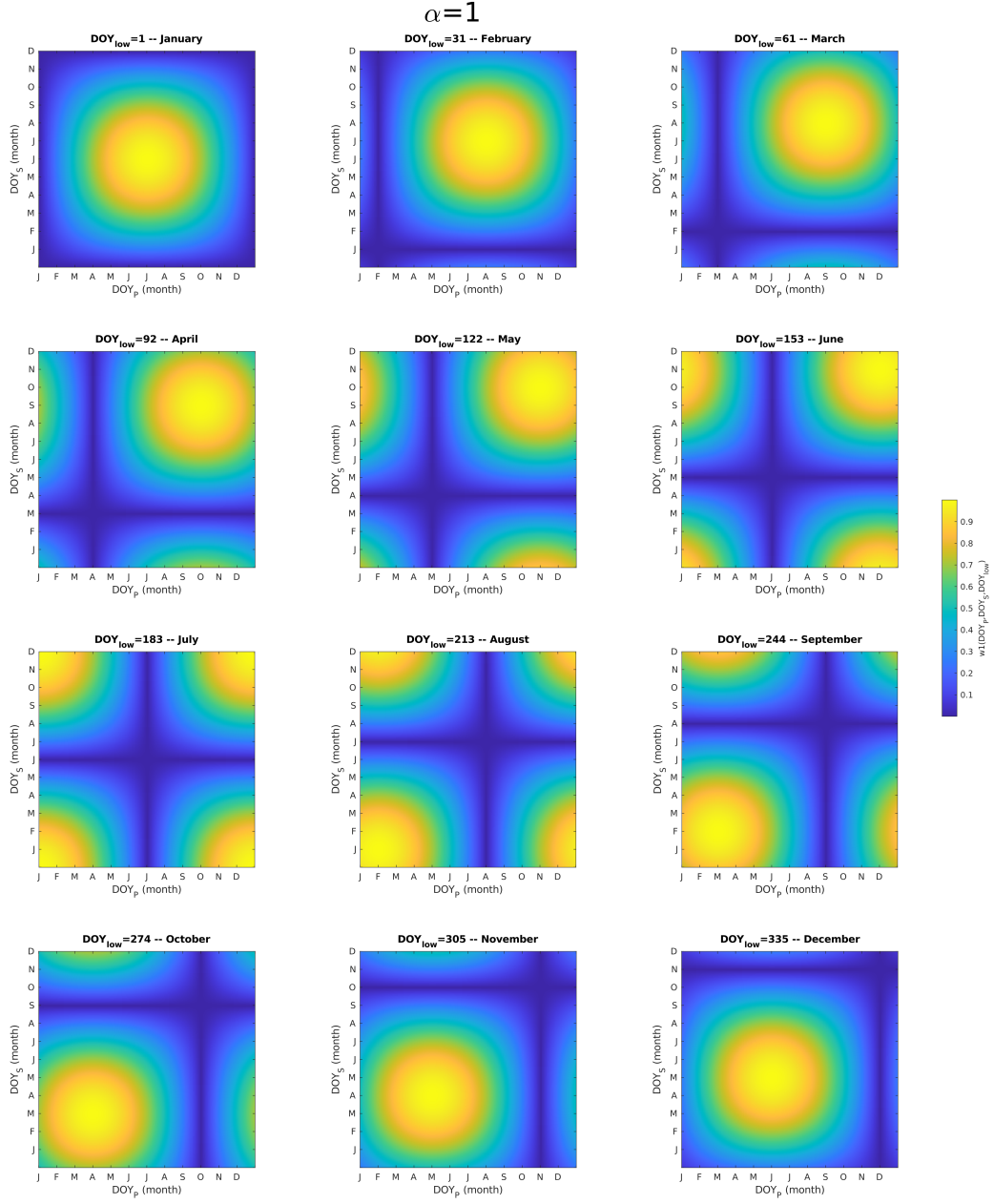


Figure S2. Evolution of the seasonal contribution $w1$ as a function of the Primary image day of year DOY_P and Secondary image day of year DOY_S for 12 values of the lowest coherence day of year DOY_{low} corresponding to the beginning of each month and the calibration factor $\alpha = 1$.

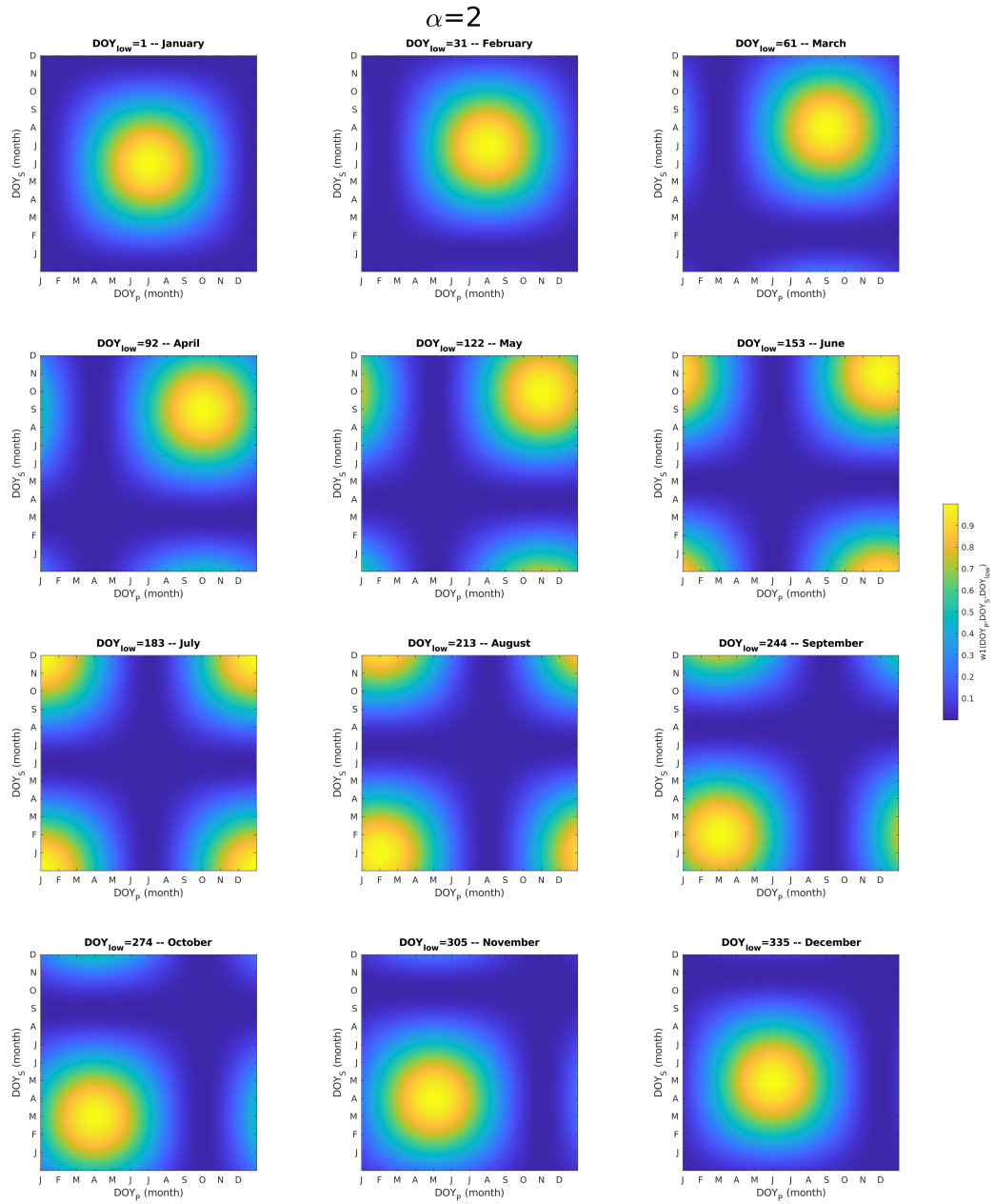


Figure S3. Evolution of the seasonal contribution $w1$ as a function of the Primary image day of year DOY_P and Secondary image day of year DOY_S for 12 values of the lowest coherence day of year DOY_{low} corresponding to the beginning of each month and the calibration factor $\alpha = 2$.

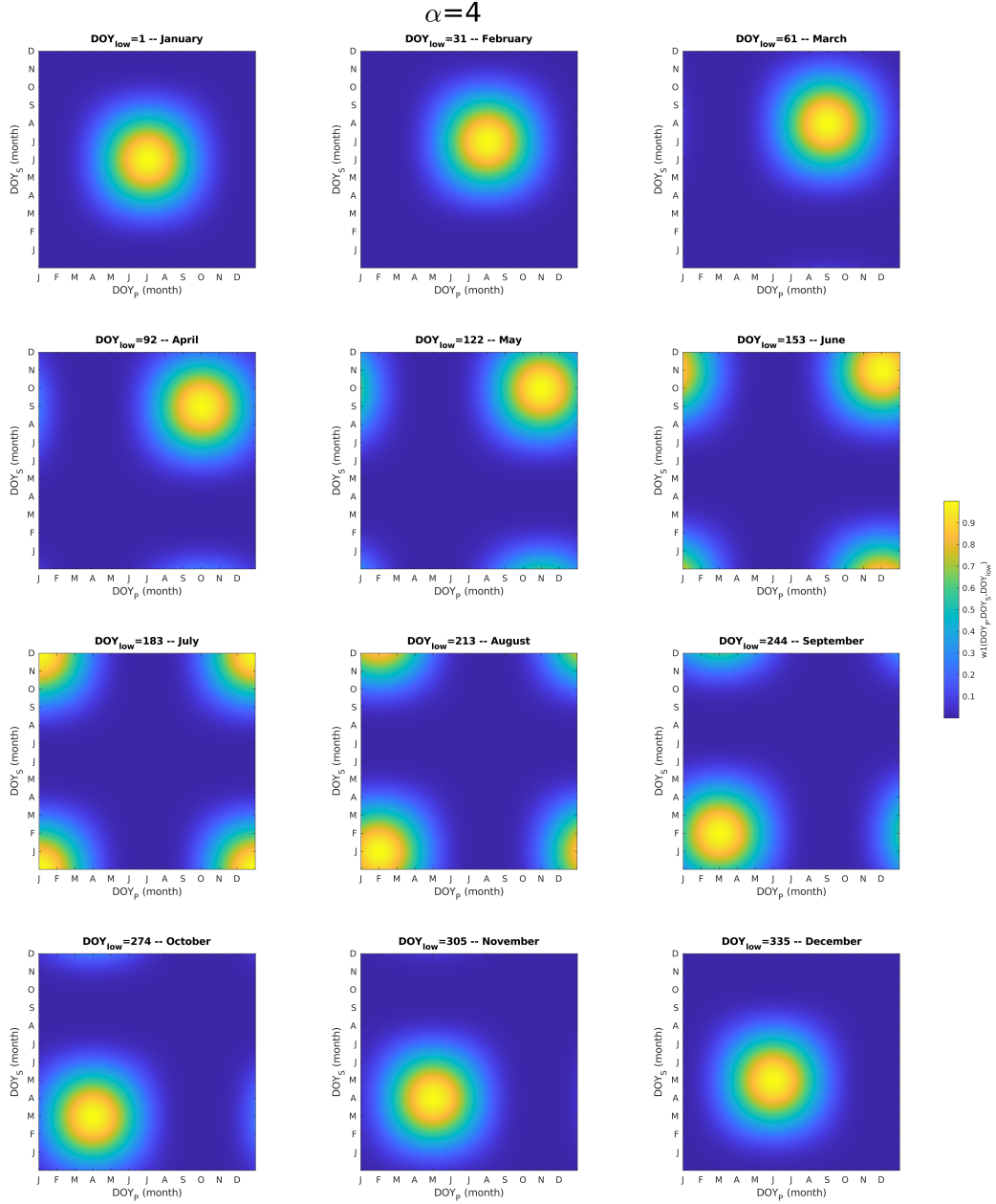


Figure S4. Evolution of the seasonal contribution $w1$ as a function of the Primary image day of year DOY_P and Secondary image day of year DOY_S for 12 values of the lowest coherence day of year DOY_{low} corresponding to the beginning of each month and the calibration factor $\alpha = 4$.

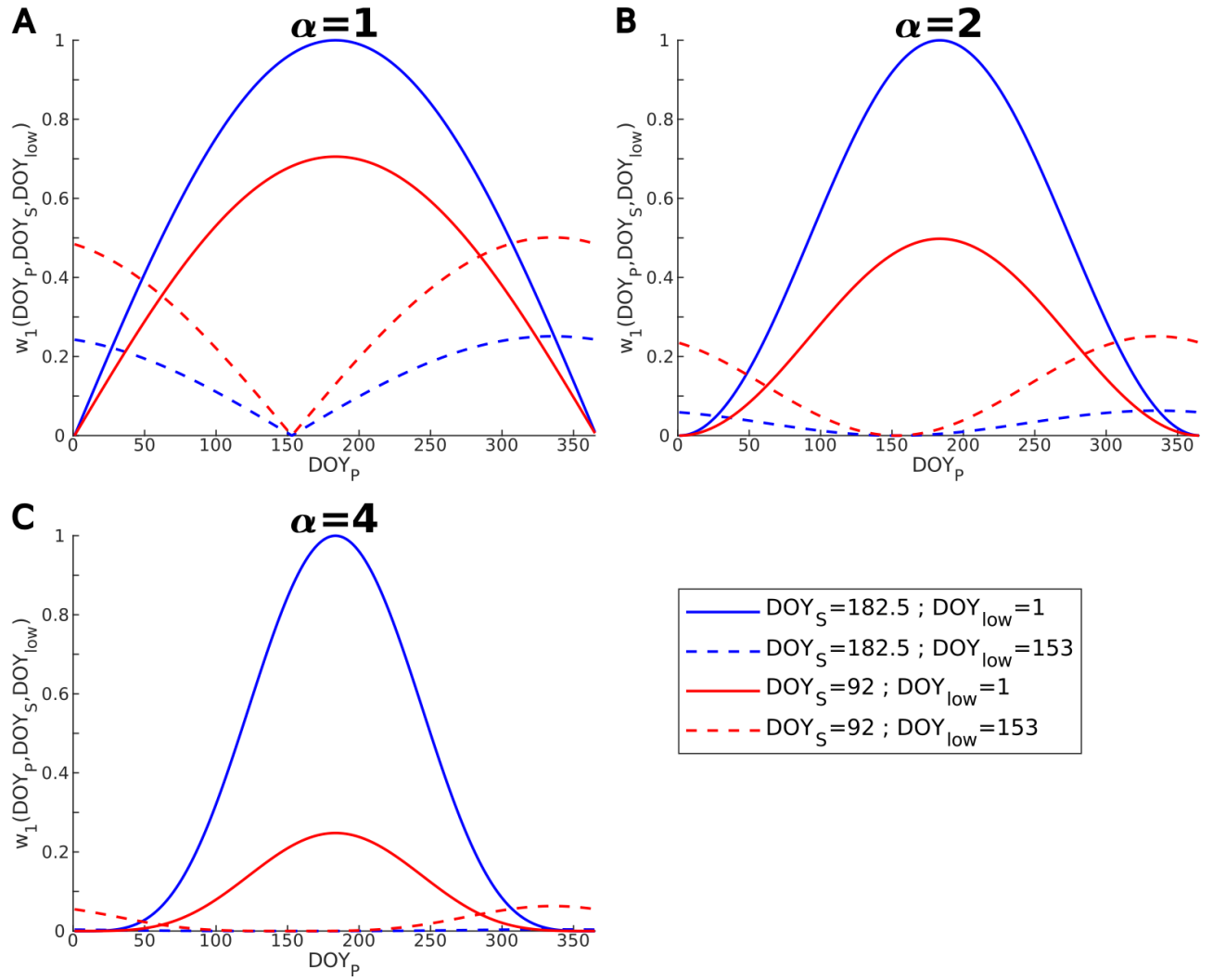


Figure S5. Evolution of the seasonal contribution w_1 as a function of the Primary image day of year DOY_P for (A) $\alpha = 1$, (B) $\alpha = 2$ and (C) $\alpha = 4$. The Secondary image acquisition are fixed to April 2nd ($DOY_S = 92$) in red or July 1st ($DOY_S = 182.5$) in blue. The day of year with the lowest coherence is chosen as January 1st ($DOY_{low} = 1$) in plain lines or June 2nd ($DOY_{low} = 153$) in dashed lines.

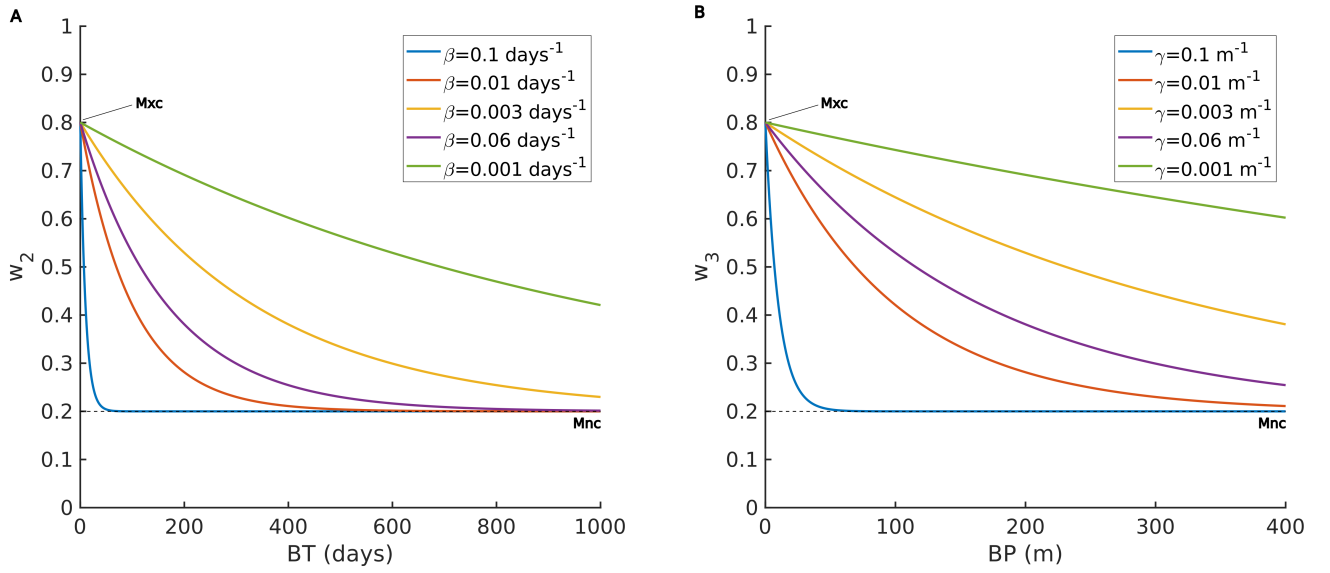


Figure S6. Evolution of temporal and spatial contributions to the coherence proxy. (A) Evolution of the temporal contribution w_2 as a function of the temporal baseline BT for several values of the calibration parameter β . (B) Evolution of the spatial contribution w_3 as a function of the perpendicular baseline BP for several values of the calibration parameter γ . M_{xc} and M_{nc} are the maximum and minimum values expected for mean the coherence in the region of interest.

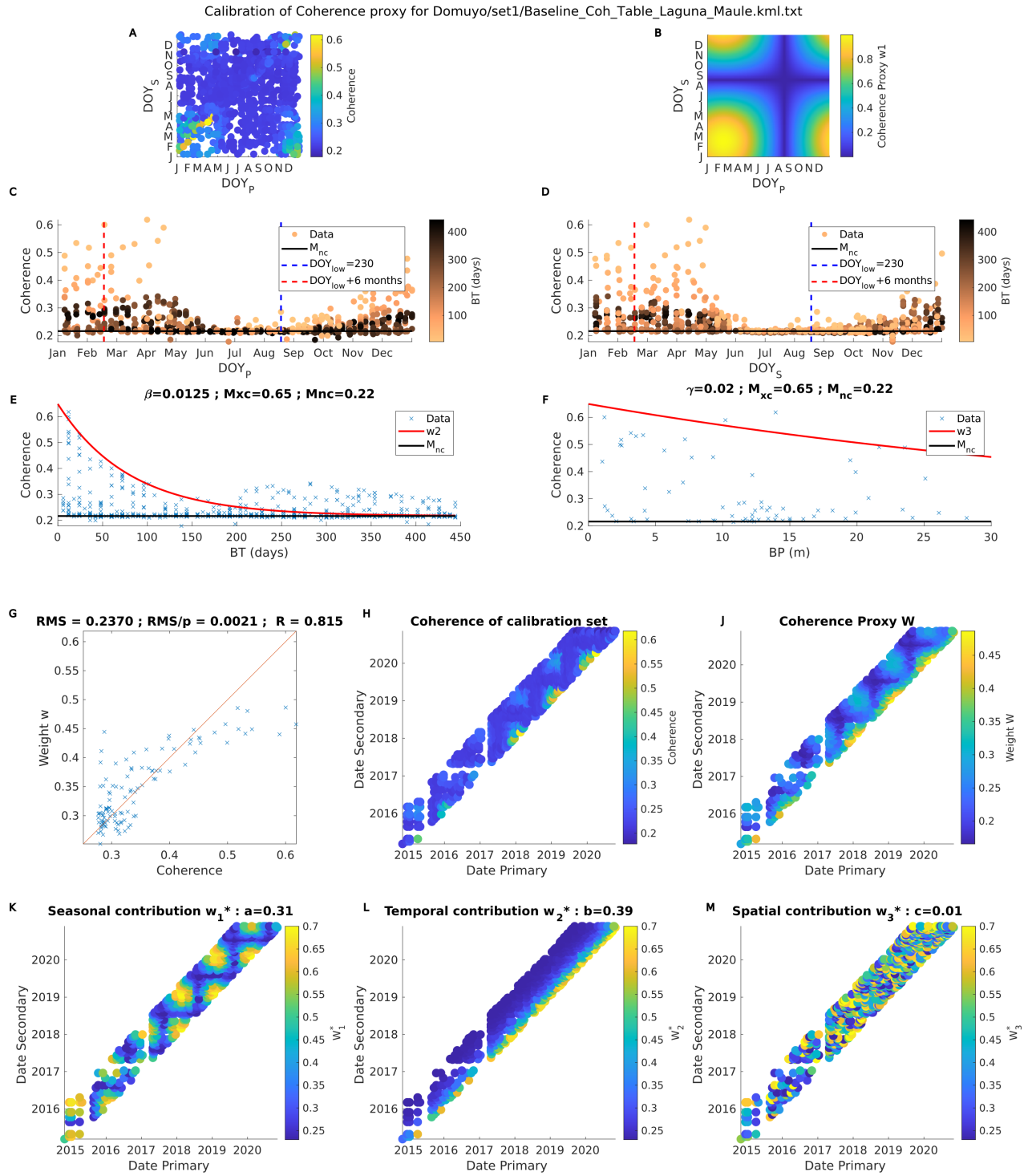


Figure S7. Calibration of the coherence proxy on the DLM area for S1 ascending dataset. A and B represent the mean coherence computed on the Laguna del Maule ROI and the seasonal contribution w_1 to the coherence proxy as a function of the primary and secondary image day of year of each pair. C and D represent the mean coherence computed on the Laguna del Maule ROI as a function of the Primary (Secondary) image Day of year respectively. Blue and red dash lines mark DOY_{low} and $DOY_{low} + 6$ months, respectively. E and F represent the mean coherence computed on the Laguna del Maule ROI as a function of BT for pairs with $BP < 15$ m and as a function of BP for pairs with $BT < 25$ days, respectively. Red line represent the exponential decrease modeled by w_2 and w_3 in the coherence proxy. C to F, horizontal black line marks the minimum expected value of the coherence M_{nc} . G represents the coherence proxy w versus the mean coherence computed on the Laguna del Maule ROI for each pair of the calibration set. The red line marks the first bisector. H and J represent the the mean coherence computed on the Laguna del Maule ROI for each pair of the calibration set and the coherence proxy w , respectively, as a function of the primary and secondary image acquisition date. K to M, the color scale represent the partial weights w_1 , w_2 and w_3 (see text section 2.3.1.2), respectively. The value of the corresponding coefficients a , b , and c is indicated on top of each plot.

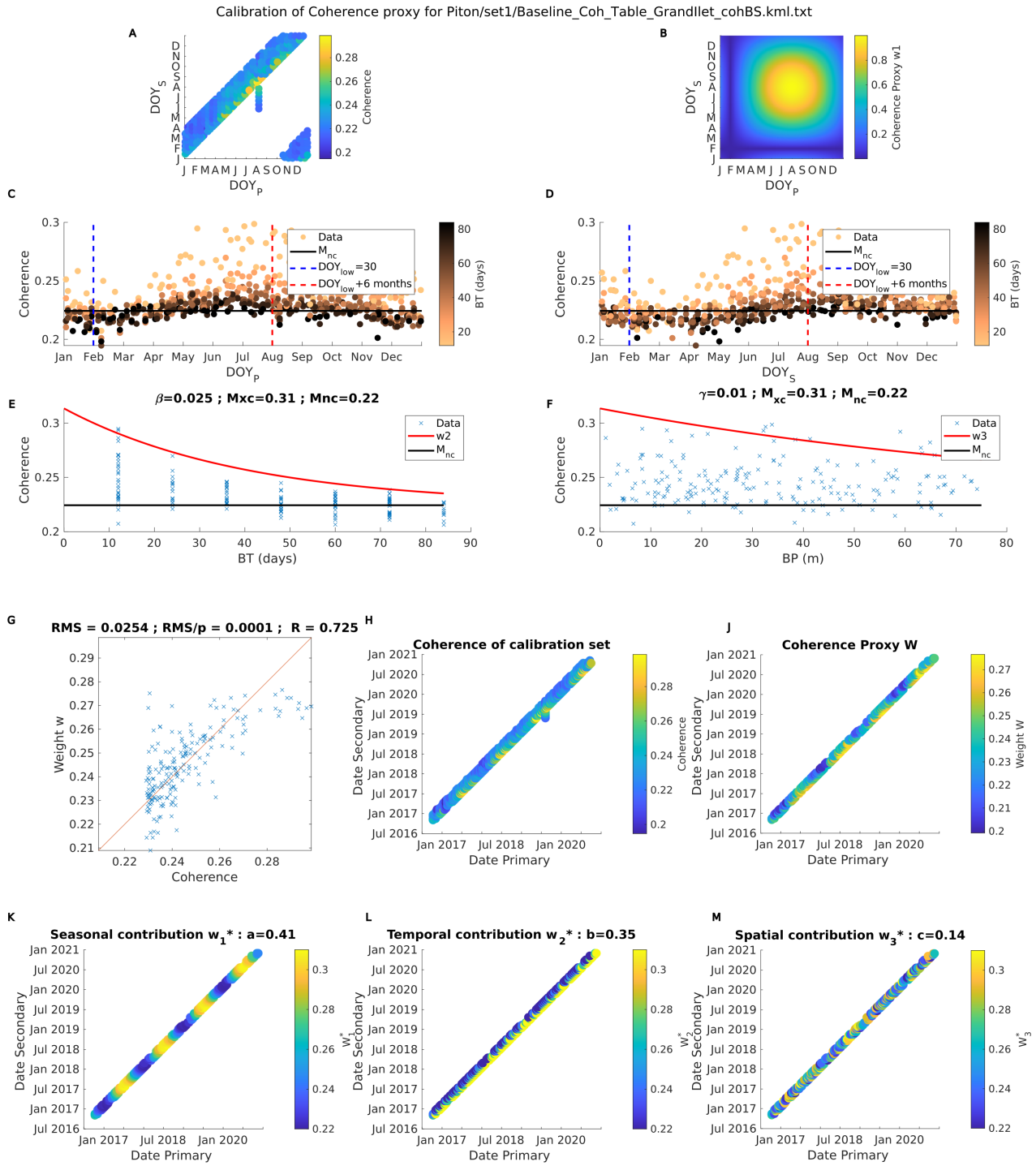


Figure S8. Calibration of the coherence proxy on the Reunion Island area for S1 SM ascending dataset. A and B represent the mean coherence computed on the Grand Ilet ROI and the seasonal contribution w_1 to the coherence proxy as a function of the primary and secondary image day of year of each pair. C and D represent the mean coherence computed on the Grand Ilet ROI as a function of the Primary (Secondary) image Day of year respectively. Blue and red dash lines mark DOY_{low} and $DOY_{low} + 6$ months, respectively. E and F represent the mean coherence computed on the Grand Ilet ROI as a function of BT for pairs with $BP < 15$ m and as a function of BP for pairs with $BT < 25$ days, respectively. Red line represent the exponential decrease modeled by w_2 and w_3 in the coherence proxy. C to F, horizontal black line marks the minimum expected value of the coherence M_{nc} . G represents the coherence proxy w versus the mean coherence computed on the Grand Ilet ROI for each pair of the calibration set. The red line marks the first bisector. H and J represent the mean coherence computed on the Grand Ilet ROI for each pair of the calibration set and the coherence proxy w , respectively, as a function of the primary and secondary image acquisition date. K to M, the color scale represent the partial weights w_1 , w_2 and w_3 (see text section 2.3.1.2), respectively. The value of the corresponding coefficients a , b , and c is indicated on top of each plot.

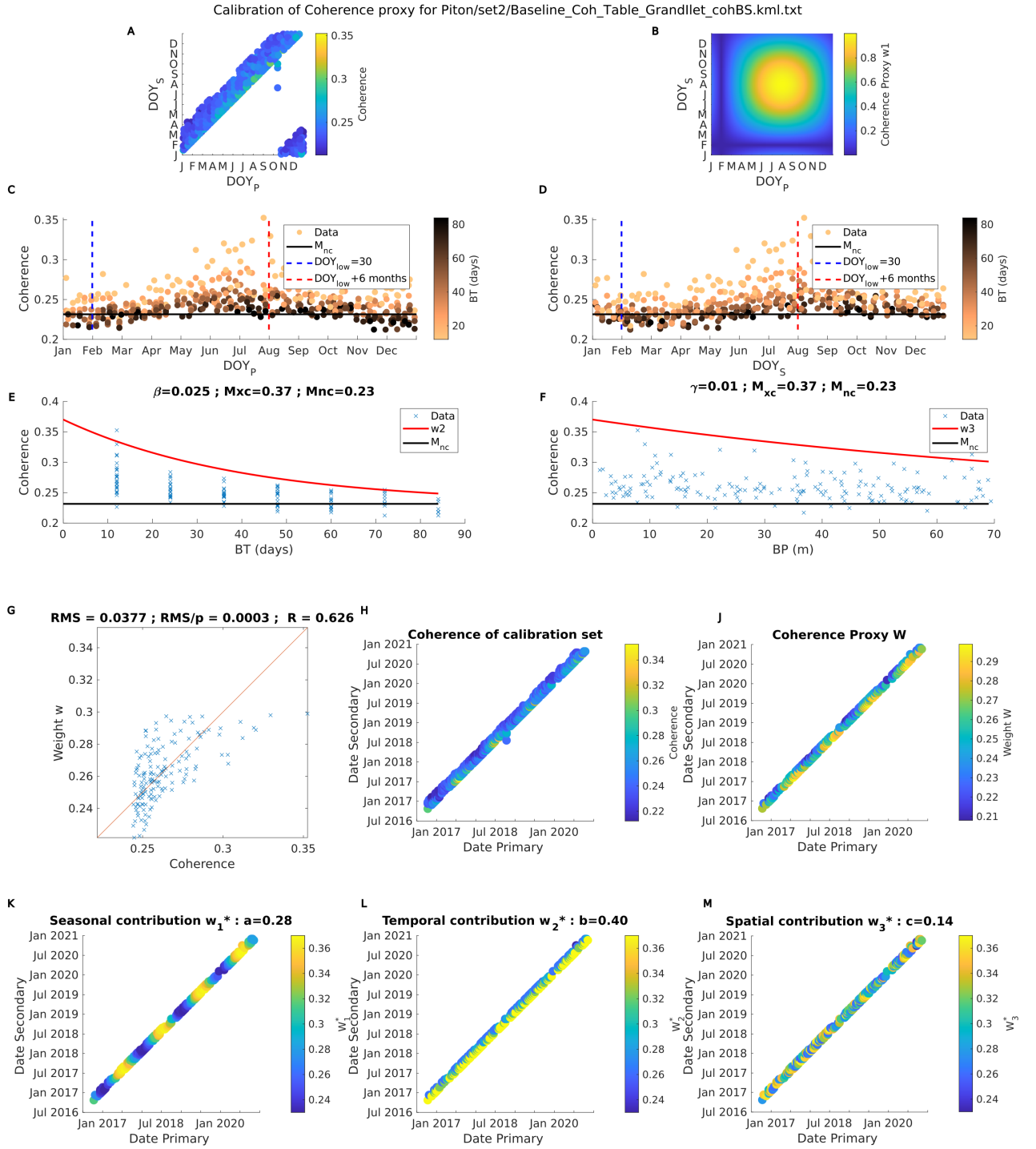


Figure S9. Calibration of the coherence proxy on the Reunion Island area for S1 SM descending dataset. A and B represent the mean coherence computed on the Grand Ilet ROI and the seasonal contribution w_1 to the coherence proxy as a function of the primary and secondary image day of year of each pair. C and D represent the mean coherence computed on the Grand Ilet ROI as a function of the Primary (Secondary) image Day of year respectively. Blue and red dash lines mark DOY_{low} and $DOY_{low} + 6$ months, respectively. E and F represent the mean coherence computed on the Grand Ilet ROI as a function of BT for pairs with $BP < 15$ m and as a function of BP for pairs with $BT < 25$ days, respectively. Red line represent the exponential decrease modeled by w_2 and w_3 in the coherence proxy. C to F, horizontal black line marks the minimum expected value of the coherence M_{nc} . G represents the coherence proxy w versus the mean coherence computed on the Grand Ilet ROI for each pair of the calibration set. The red line marks the first bisector. H and J represent the mean coherence computed on the Grand Ilet ROI for each pair of the calibration set and the coherence proxy w , respectively, as a function of the primary and secondary image acquisition date. K to M, the color scale represent the partial weights w_1 , w_2 and w_3 (see text section 2.3.1.2), respectively. The value of the corresponding coefficients a , b , and c is indicated on top of each plot.

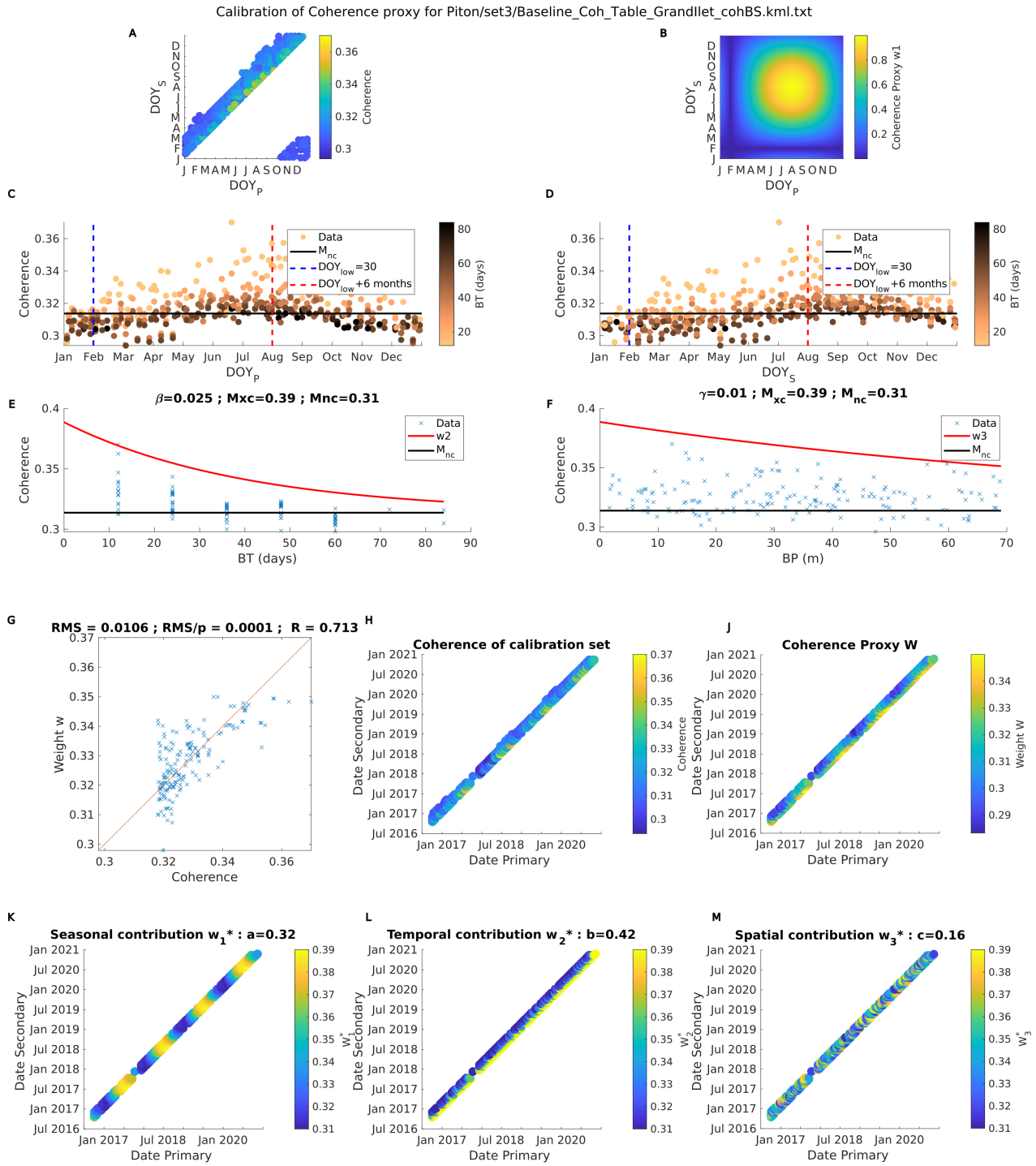


Figure S10. Calibration of the coherence proxy on the Reunion Island area for S1 IW ascending dataset. A and B represent the mean coherence computed on the Grand Ilet ROI and the seasonal contribution w_1 to the coherence proxy as a function of the primary and secondary image day of year of each pair. C and D represent the mean coherence computed on the Grand Ilet ROI as a function of the Primary (Secondary) image Day of year respectively. Blue and red dash lines mark DOY_{low} and $DOY_{low} + 6$ months, respectively. E and F represent the mean coherence computed on the Grand Ilet ROI as a function of BT for pairs with $BP < 15$ m and as a function of BP for pairs with $BT < 25$ days, respectively. Red line represent the exponential decrease modeled by w_2 and w_3 in the coherence proxy. C to F, horizontal black line marks the minimum expected value of the coherence M_{nc} . G represents the coherence proxy w versus the mean coherence computed on the Grand Ilet ROI for each pair of the calibration set. The red line marks the first bisector. H and J represent the mean coherence computed on the Grand Ilet ROI for each pair of the calibration set and the coherence proxy w , respectively, as a function of the primary and secondary image acquisition date. K to M, the color scale represent the partial weights w_1 , w_2 and w_3 (see text section 2.3.1.2), respectively. The value of the corresponding coefficients a , b , and c is indicated on top of each plot.

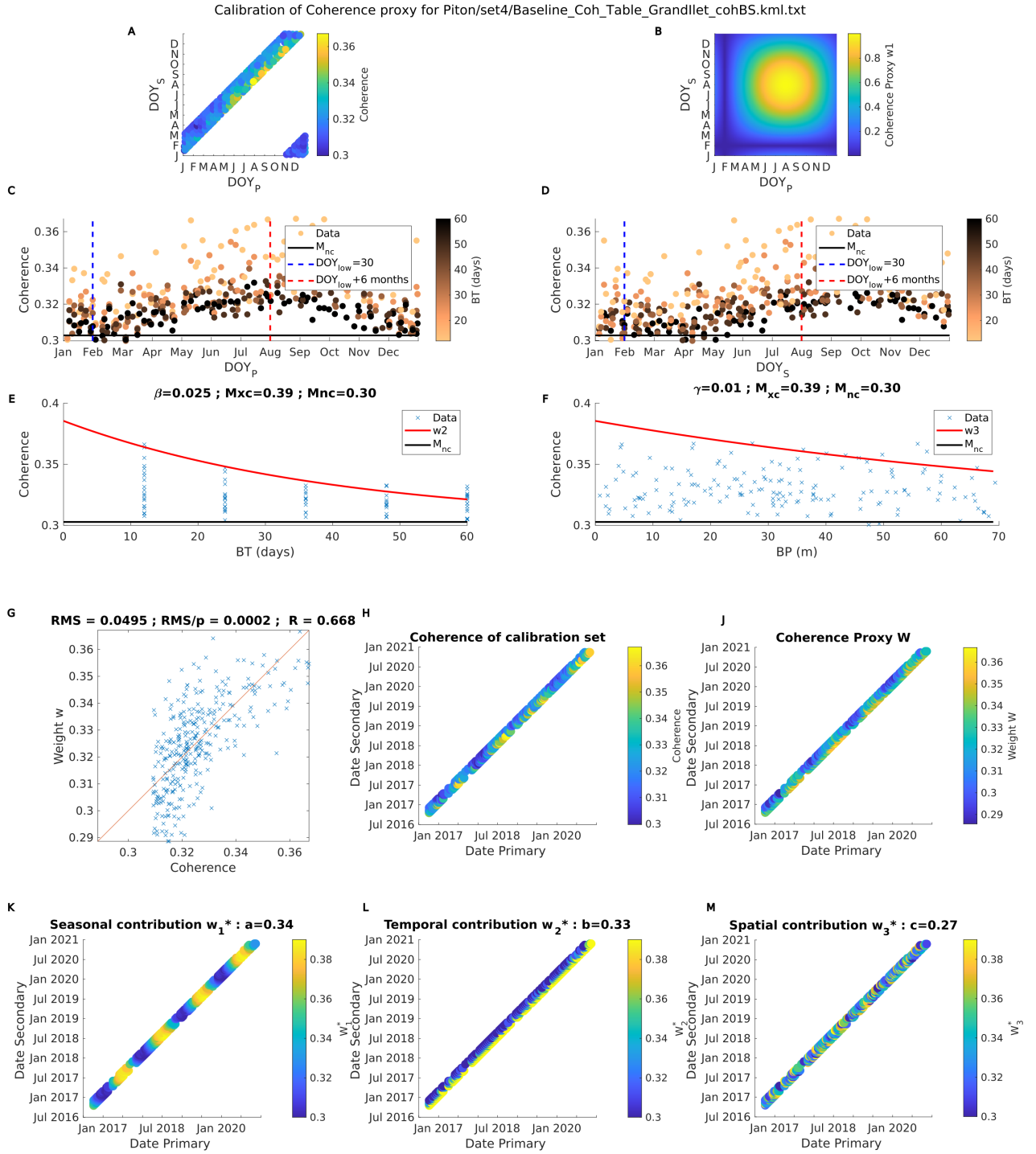


Figure S11. Calibration of the coherence proxy on the Reunion Island area for S1 IW descending dataset. A and B represent the mean coherence computed on the Grand Ilet ROI and the seasonal contribution w_1 to the coherence proxy as a function of the primary and secondary image day of year of each pair. C and D represent the mean coherence computed on the Grand Ilet ROI as a function of the Primary (Secondary) image Day of year respectively. Blue and red dash lines mark DOY_{low} and $DOY_{low} + 6$ months, respectively. E and F represent the mean coherence computed on the Grand Ilet ROI as a function of BT for pairs with $BP < 15$ m and as a function of BP for pairs with $BT < 25$ days, respectively. Red line represent the exponential decrease modeled by w_2 and w_3 in the coherence proxy. C to F, horizontal black line marks the minimum expected value of the coherence M_{nc} . G represents the coherence proxy w versus the mean coherence computed on the Grand Ilet ROI for each pair of the calibration set. The red line marks the first bisector. H and J represent the mean coherence computed on the Grand Ilet ROI for each pair of the calibration set and the coherence proxy w , respectively, as a function of the primary and secondary image acquisition date. K to M, the color scale represent the partial weights w_1 , w_2 and w_3 (see text section 2.3.1.2), respectively. The value of the corresponding coefficients a , b , and c is indicated on top of each plot.

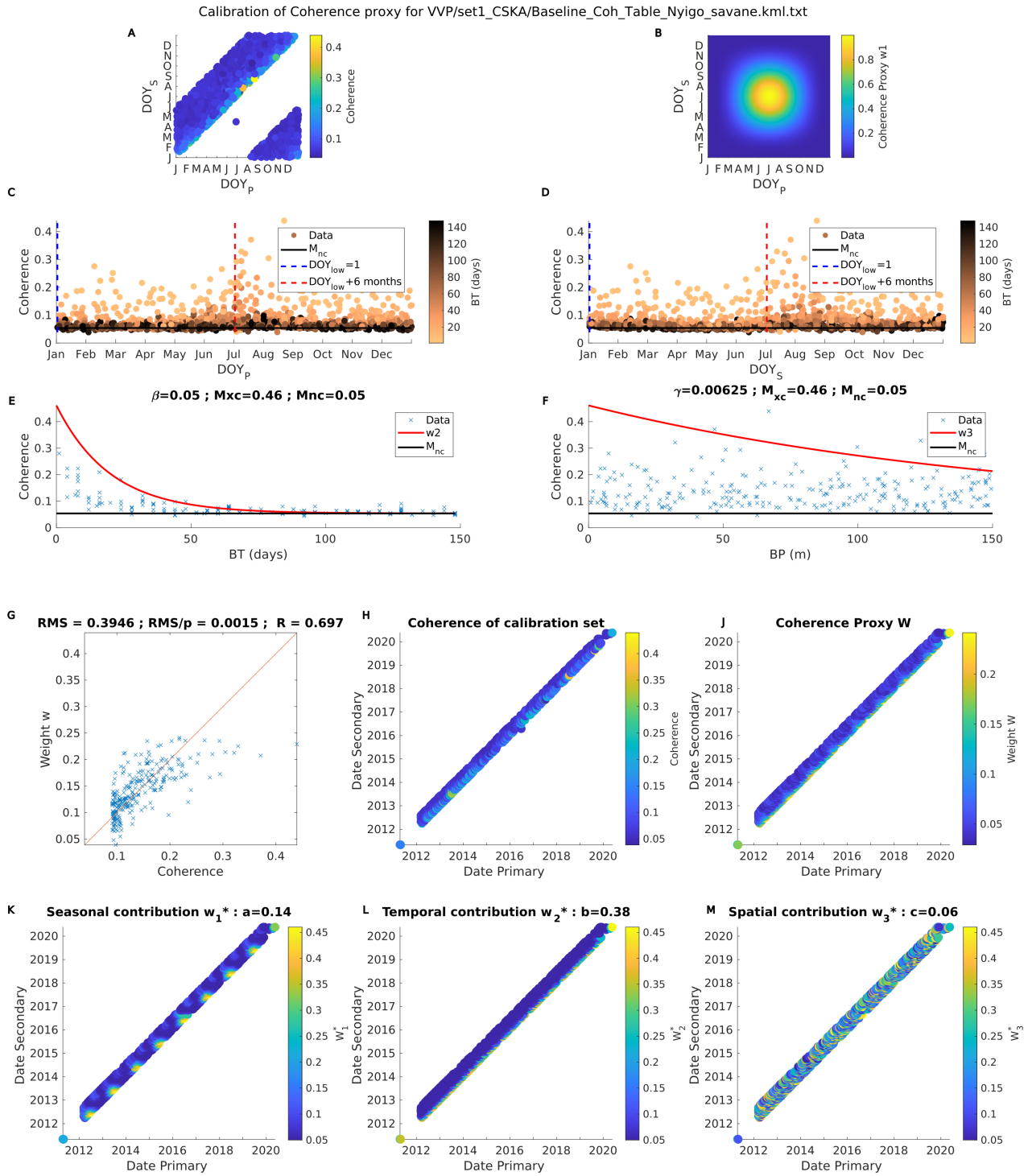


Figure S12. Calibration of the coherence proxy on the VVP area for CSK ascending dataset. A and B represent the mean coherence computed on the Savannah ROI and the seasonal contribution w_1 to the coherence proxy as a function of the primary and secondary image day of year of each pair. C and D represent the mean coherence computed on the Savannah ROI as a function of the Primary (Secondary) image Day of year respectively. Blue and red dash lines mark DOY_{low} and $DOY_{low} + 6$ months, respectively. E and F represent the mean coherence computed on the Savannah ROI as a function of BT for pairs with $BP < 15$ m and as a function of BP for pairs with $BT < 25$ days, respectively. Red line represent the exponential decrease modeled by w_2 and w_3 in the coherence proxy. C to F, horizontal black line marks the minimum expected value of the coherence M_{nc} . G represents the coherence proxy w versus the mean coherence computed on the Savannah ROI for each pair of the calibration set. The red line marks the first bisector. H and J represent the the mean coherence computed on the Savannah ROI for each pair of the calibration set and the coherence proxy w , respectively, as a function of the primary and secondary image acquisition date. K to M, the color scale represent the partial weights w_1 , w_2 and w_3 (see text section 2.3.1.2), respectively. The value of the corresponding coefficients a , b , and c is indicated on top of each plot.

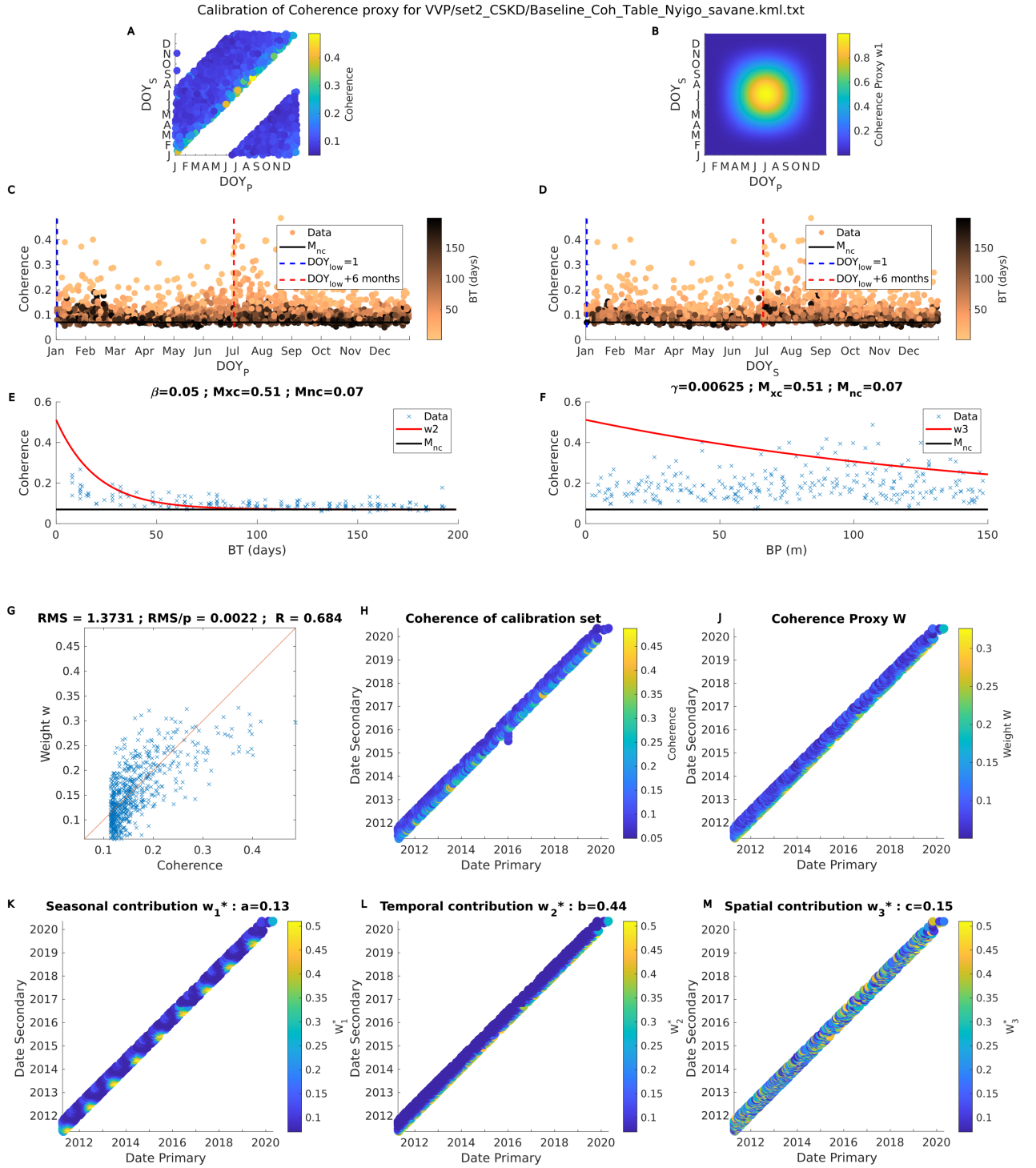


Figure S13. Calibration of the coherence proxy on the VVP area for CSK descending dataset. A and B represent the mean coherence computed on the Savannah ROI and the seasonal contribution w_1 to the coherence proxy as a function of the primary and secondary image day of year of each pair. C and D represent the mean coherence computed on the Savannah ROI as a function of the Primary (Secondary) image Day of year respectively. Blue and red dash lines mark DOY_{low} and $DOY_{low} + 6$ months, respectively. E and F represent the mean coherence computed on the Savannah ROI as a function of BT for pairs with $BP < 15$ m and as a function of BP for pairs with $BT < 25$ days, respectively. Red line represent the exponential decrease modeled by w_2 and w_3 in the coherence proxy. C to F, horizontal black line marks the minimum expected value of the coherence M_{nc} . G represents the coherence proxy w versus the mean coherence computed on the Savannah ROI for each pair of the calibration set. The red line marks the first bisector. H and J represent the the mean coherence computed on the Savannah ROI for each pair of the calibration set and the coherence proxy w , respectively, as a function of the primary and secondary image acquisition date. K to M, the color scale represent the partial weights w_1 , w_2 and w_3 (see text section 2.3.1.2), respectively. The value of the corresponding coefficients a , b , and c is indicated on top of each plot.

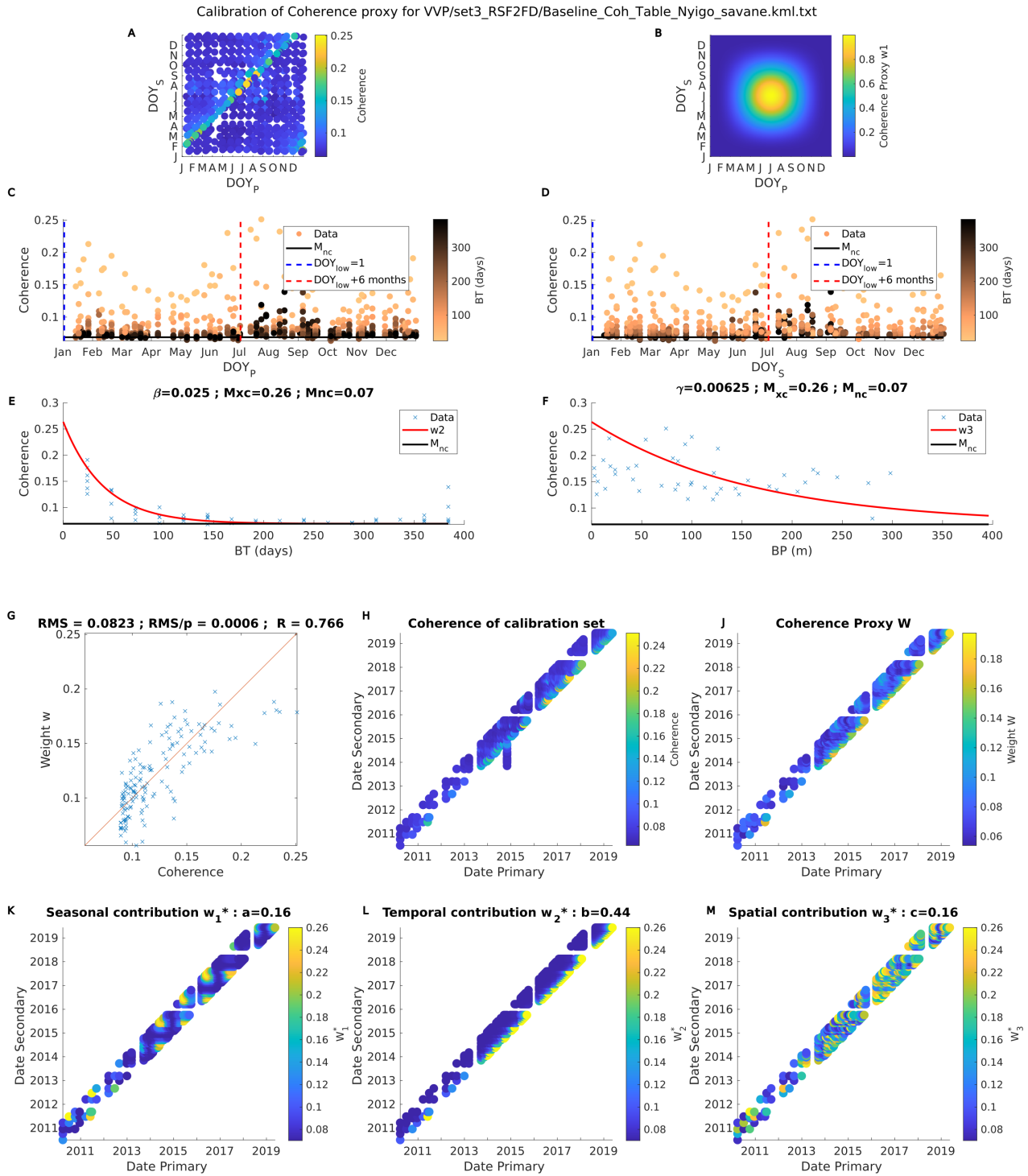


Figure S14. Calibration of the coherence proxy on the VVP area for RS F2F descending dataset. A and B represent the mean coherence computed on the Savannah ROI and the seasonal contribution w_1 to the coherence proxy as a function of the primary and secondary image day of year of each pair. C and D represent the mean coherence computed on the Savannah ROI as a function of the Primary (Secondary) image Day of year respectively. Blue and red dash lines mark DOY_{low} and $DOY_{low} + 6$ months, respectively. E and F represent the mean coherence computed on the Savannah ROI as a function of BT for pairs with $BP < 15$ m and as a function of BP for pairs with $BT < 25$ days, respectively. Red line represent the exponential decrease modeled by w_2 and w_3 in the coherence proxy. C to F, horizontal black line marks the minimum expected value of the coherence M_{nc} . G represents the coherence proxy w versus the mean coherence computed on the Savannah ROI for each pair of the calibration set. The red line marks the first bisector. H and J represent the the mean coherence computed on the Savannah ROI for each pair of the calibration set and the coherence proxy w , respectively, as a function of the primary and secondary image acquisition date. K to M, the color scale represent the partial weights w_1 , w_2 and w_3 (see text section 2.3.1.2), respectively. The value of the corresponding coefficients a , b , and c is indicated on top of each plot.

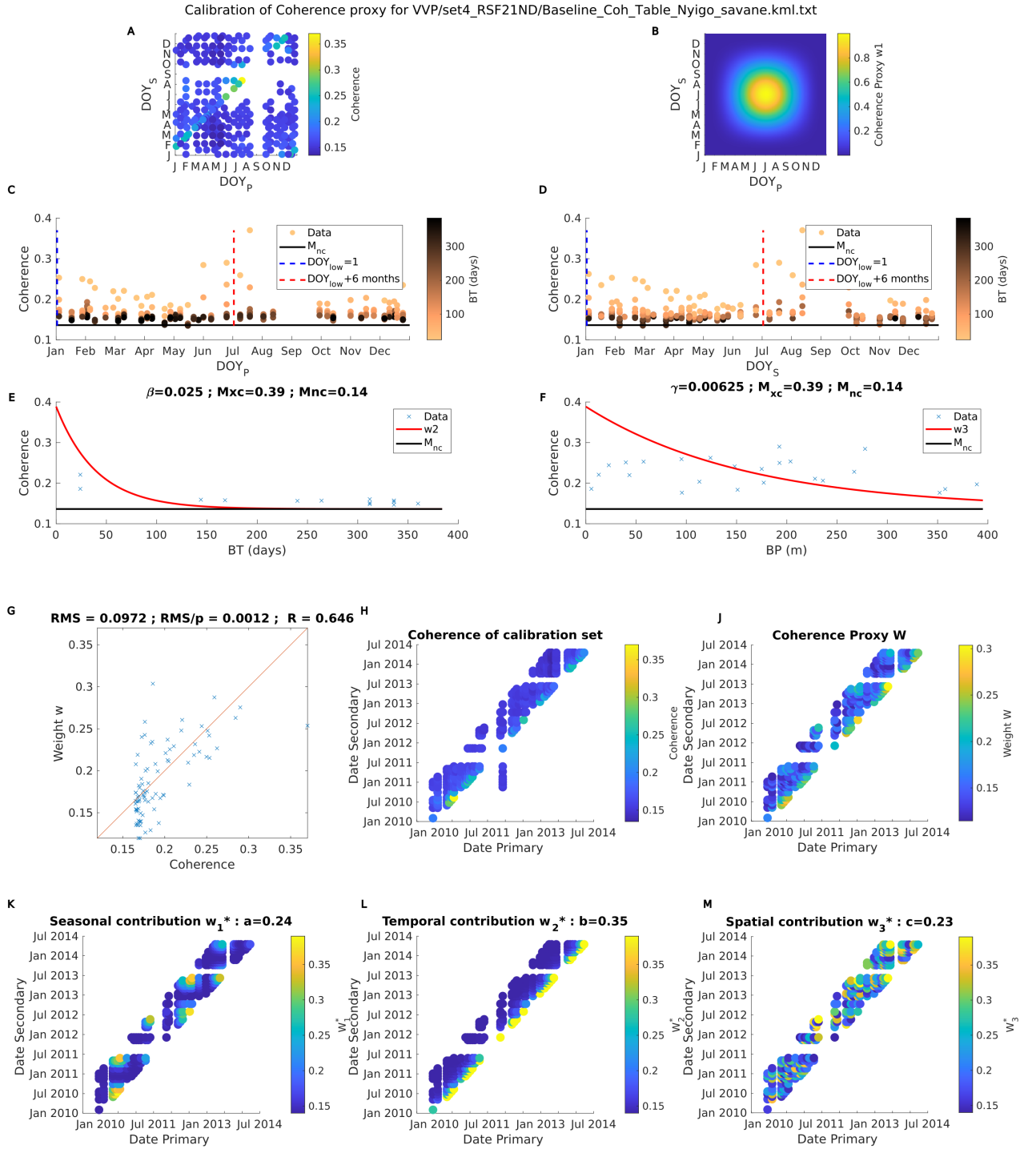


Figure S15. Calibration of the coherence proxy on the VVP area for RS F21N descending dataset. A and B represent the mean coherence computed on the Savannah ROI and the seasonal contribution w_1 to the coherence proxy as a function of the primary and secondary image day of year of each pair. C and D represent the mean coherence computed on the Savannah ROI as a function of the Primary (Secondary) image Day of year respectively. Blue and red dash lines mark DOY_{low} and $DOY_{low} + 6$ months, respectively. E and F represent the mean coherence computed on the Savannah ROI as a function of BT for pairs with $BP < 15$ m and as a function of BP for pairs with $BT < 25$ days, respectively. Red line represent the exponential decrease modeled by w_2 and w_3 in the coherence proxy. C to F, horizontal black line marks the minimum expected value of the coherence M_{nc} . G represents the coherence proxy w versus the mean coherence computed on the Savannah ROI for each pair of the calibration set. The red line marks the first bisector. H and J represent the the mean coherence computed on the Savannah ROI for each pair of the calibration set and the coherence proxy w , respectively, as a function of the primary and secondary image acquisition date. K to M, the color scale represent the partial weights w_1 , w_2 and w_3 (see text section 2.3.1.2), respectively. The value of the corresponding coefficients a , b , and c is indicated on top of each plot.

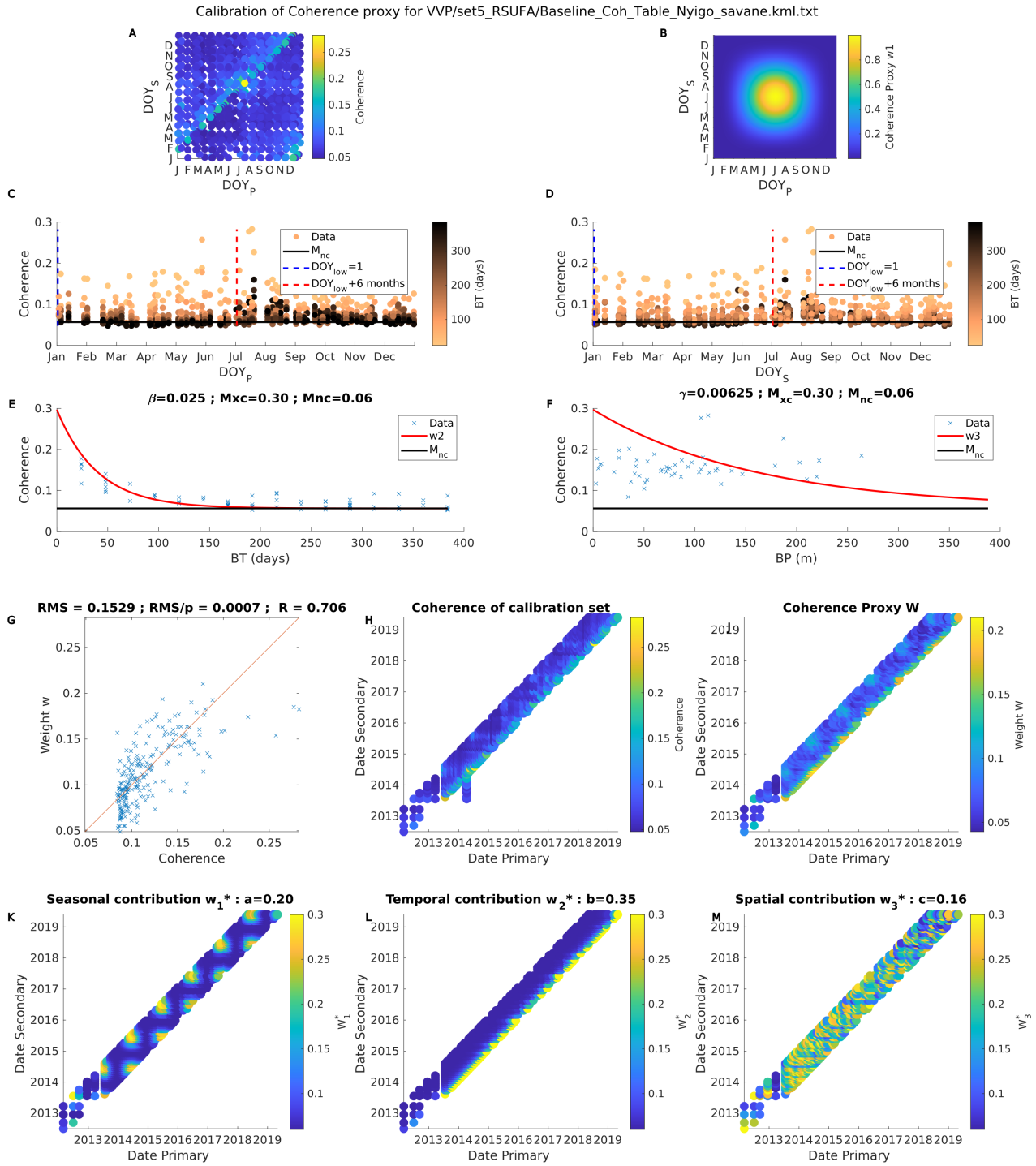


Figure S16. Calibration of the coherence proxy on the VVP area for RS UF ascending dataset. A and B represent the mean coherence computed on the Savannah ROI and the seasonal contribution w_1 to the coherence proxy as a function of the primary and secondary image day of year of each pair. C and D represent the mean coherence computed on the Savannah ROI as a function of the Primary (Secondary) image Day of year respectively. Blue and red dash lines mark DOY_{low} and $DOY_{low} + 6$ months, respectively. E and F represent the mean coherence computed on the Savannah ROI as a function of BT for pairs with $BP < 15$ m and as a function of BP for pairs with $BT < 25$ days, respectively. Red line represent the exponential decrease modeled by w_2 and w_3 in the coherence proxy. C to F, horizontal black line marks the minimum expected value of the coherence M_{nc} . G represents the coherence proxy w versus the mean coherence computed on the Savannah ROI for each pair of the calibration set. The red line marks the first bisector. H and I represent the the mean coherence computed on the Savannah ROI for each pair of the calibration set and the coherence proxy w , respectively, as a function of the primary and secondary image acquisition date. K to M, the color scale represent the partial weights w_1 , w_2 and w_3 (see text section 2.3.1.2), respectively. The value of the corresponding coefficients a , b , and c is indicated on top of each plot.

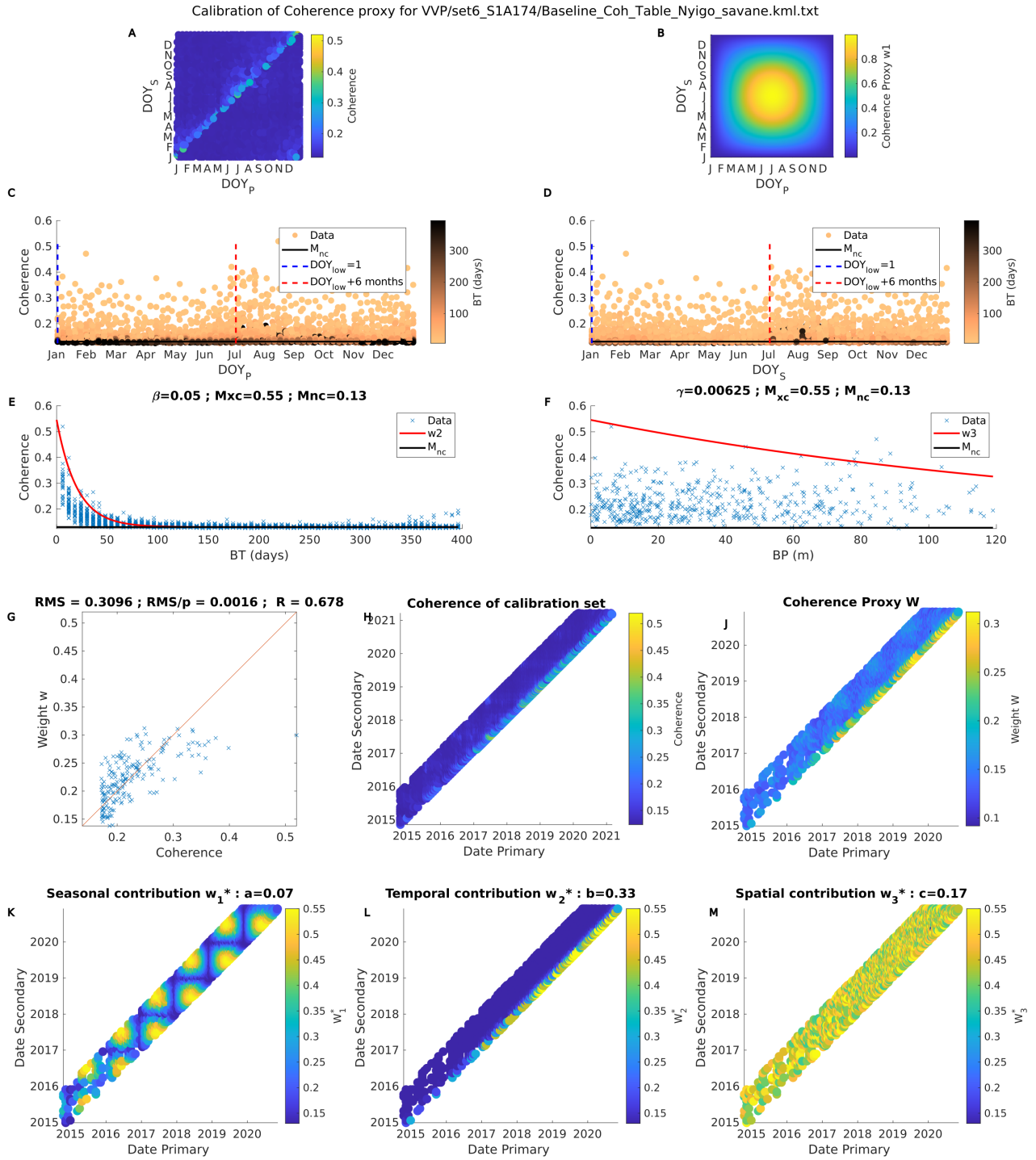


Figure S17. Calibration of the coherence proxy on the VVP area for S1 ascending dataset. A and B represent the mean coherence computed on the Savannah ROI and the seasonal contribution w_1 to the coherence proxy as a function of the primary and secondary image day of year of each pair. C and D represent the mean coherence computed on the Savannah ROI as a function of the Primary (Secondary) image Day of year respectively. Blue and red dash lines mark DOY_{low} and $DOY_{low} + 6$ months, respectively. E and F represent the mean coherence computed on the Savannah ROI as a function of BT for pairs with $BP < 15$ m and as a function of BP for pairs with $BT < 25$ days, respectively. Red line represent the exponential decrease modeled by w_2 and w_3 in the coherence proxy. C to F, horizontal black line marks the minimum expected value of the coherence M_{nc} . G represents the coherence proxy w versus the mean coherence computed on the Savannah ROI for each pair of the calibration set. The red line marks the first bisector. H and J represent the the mean coherence computed on the Savannah ROI for each pair of the calibration set and the coherence proxy w , respectively, as a function of the primary and secondary image acquisition date. K to M, the color scale represent the partial weights w_1 , w_2 and w_3 (see text section 2.3.1.2), respectively. The value of the corresponding coefficients a , b , and c is indicated on top of each plot.

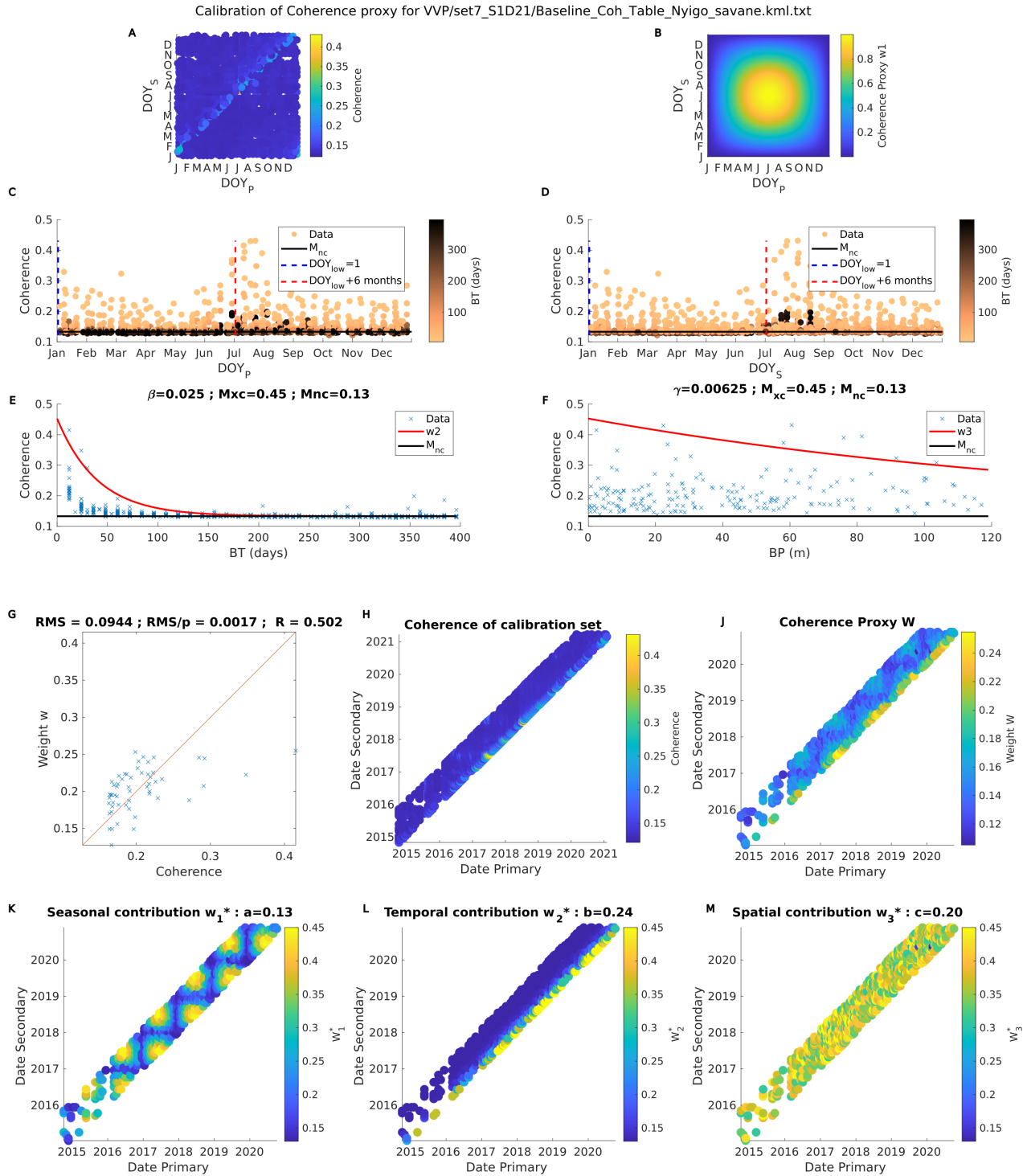


Figure S18. Calibration of the coherence proxy on the VVP area for S1 descending dataset. A and B represent the mean coherence computed on the Savannah ROI and the seasonal contribution w_1 to the coherence proxy as a function of the primary and secondary image day of year of each pair. C and D represent the mean coherence computed on the Savannah ROI as a function of the Primary (Secondary) image Day of year respectively. Blue and red dash lines mark DOY_{low} and $DOY_{low} + 6$ months, respectively. E and F represent the mean coherence computed on the Savannah ROI as a function of BT for pairs with $BP < 15$ m and as a function of BP for pairs with $BT < 25$ days, respectively. Red line represent the exponential decrease modeled by w_2 and w_3 in the coherence proxy. C to F, horizontal black line marks the minimum expected value of the coherence M_{nc} . G represents the coherence proxy w versus the mean coherence computed on the Savannah ROI for each pair of the calibration set. The red line marks the first bisector. H and J represent the the mean coherence computed on the Savannah ROI for each pair of the calibration set and the coherence proxy w , respectively, as a function of the primary and secondary image acquisition date. K to M, the color scale represent the partial weights w_1 , w_2 and w_3 (see text section 2.3.1.2), respectively. The value of the corresponding coefficients a , b , and c is indicated on top of each plot.

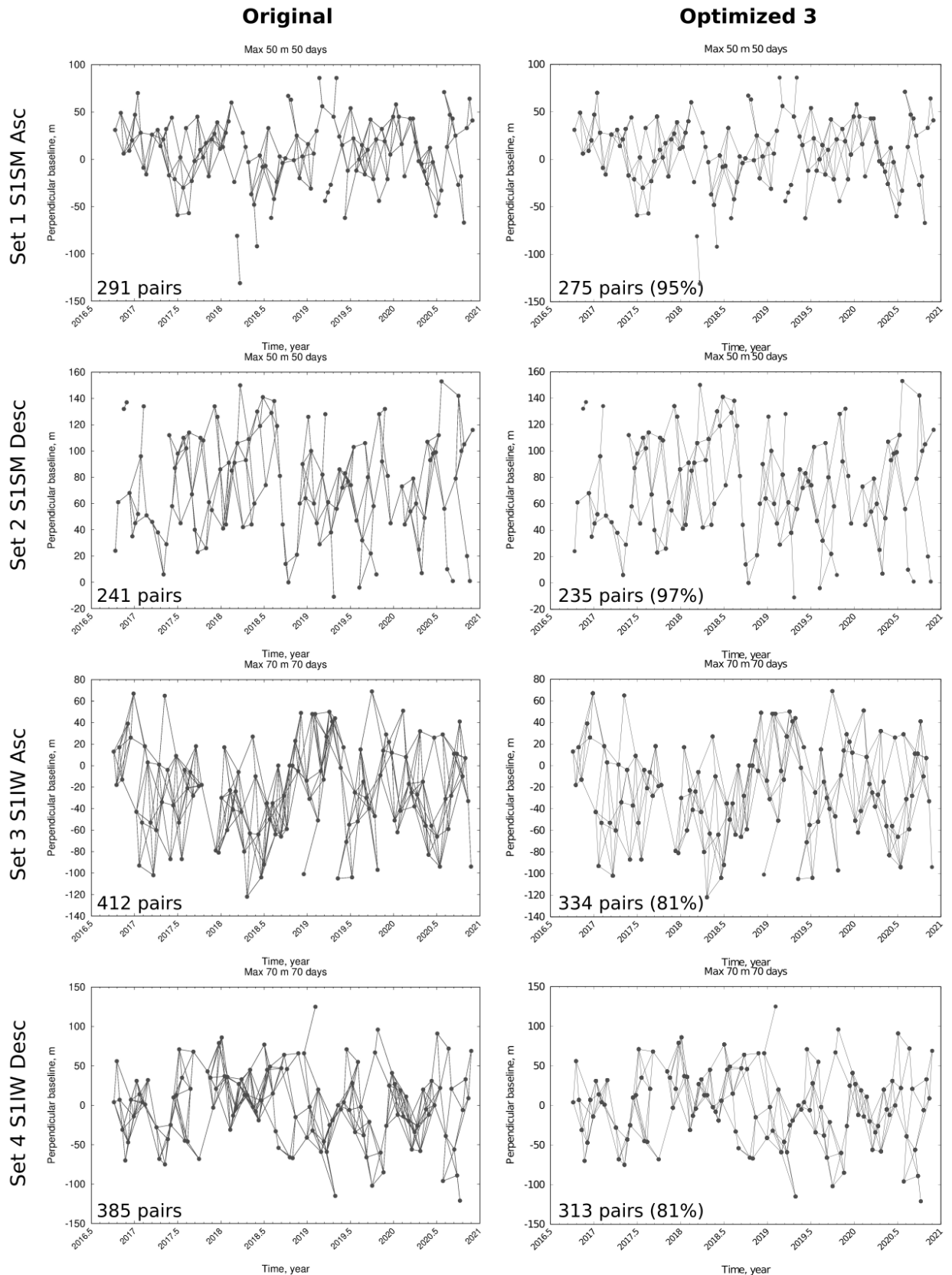


Figure S19. Original and optimized baseline plots for each S1 data set acquired on la Reunion Island. The optimization is performed with $k = 3$. The total number of pairs used is indicated in the lower left corner of each baseline plot. The percentage of pairs kept after optimization with reference to the original processing is also indicated in the optimized baselines plots. Initial baselines criteria (BP and BT) are indicated on top of each baseline plot.

November 23, 2021, 11:48am

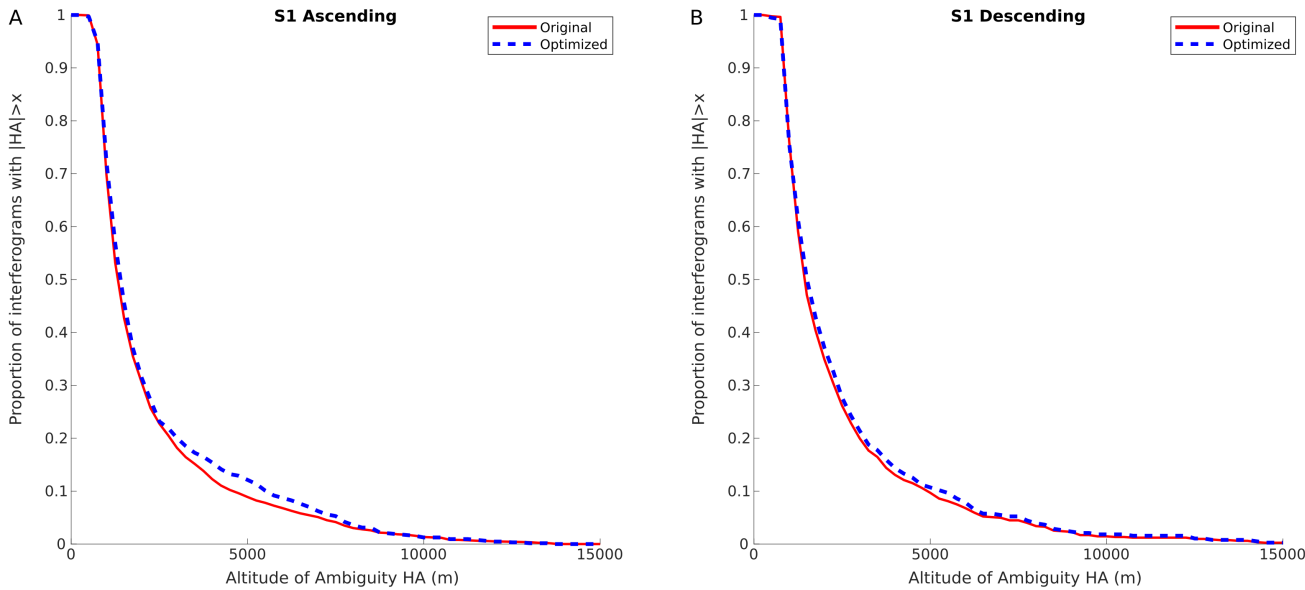


Figure S20. Proportion of interferograms in the original data set (plain red curve) and in the optimized dataset (dashed blue curve) which altitude of ambiguity is larger than a threshold as a function of the threshold. A. Sentinel 1 Ascending dataset on the VVP. B. S1 Descending dataset on the VVP.

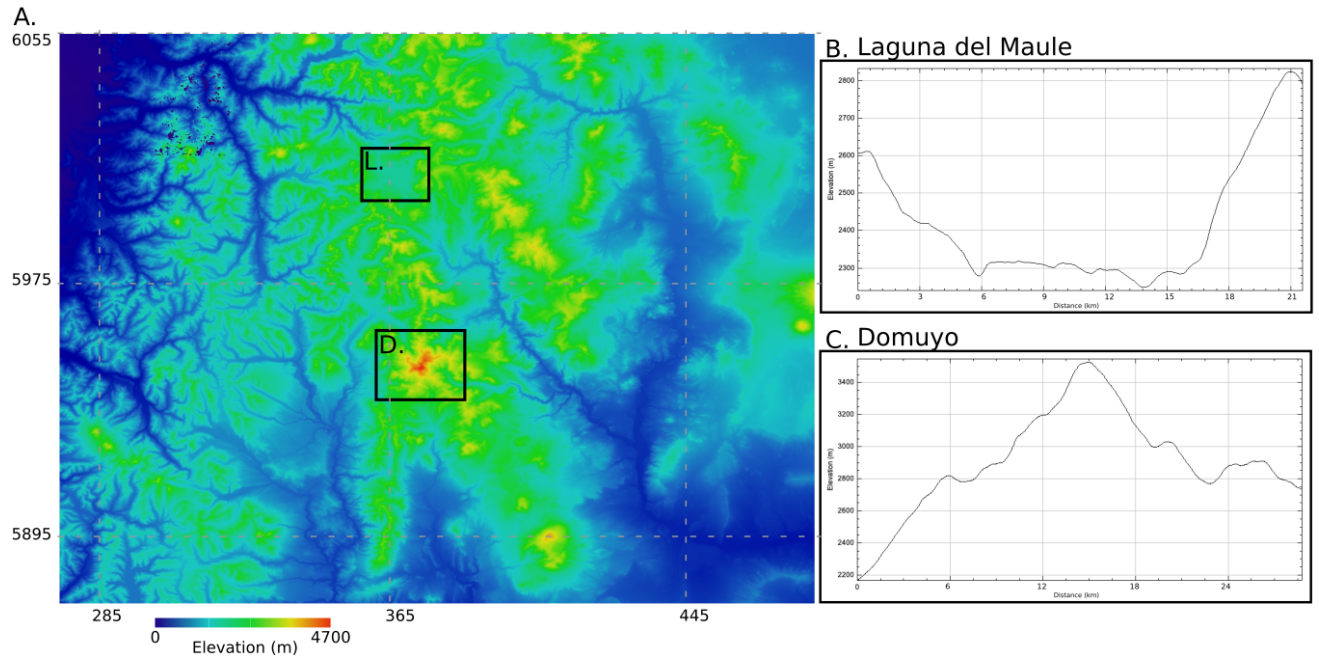


Figure S21. (A) Digital Elevation Model (SRTM 30 m) of the Domuyo and Laguna del Maule region. (B) and (C) Average East-West elevation profiles computed on the areas marked by black rectangles in (A) : the Laguna del Maule (rectangle L.) and Domuyo (rectangle D.) respectively.

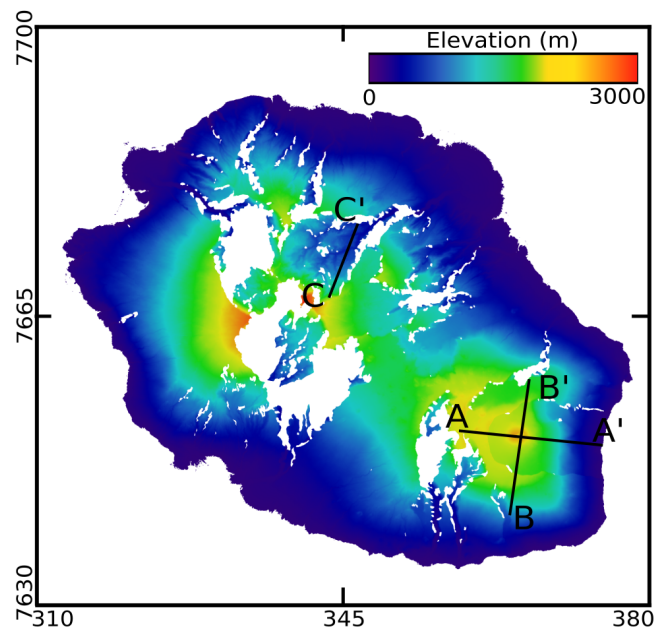


Figure S22. Digital Elevation Model (SRTM 30 m) of the Reunion Island.

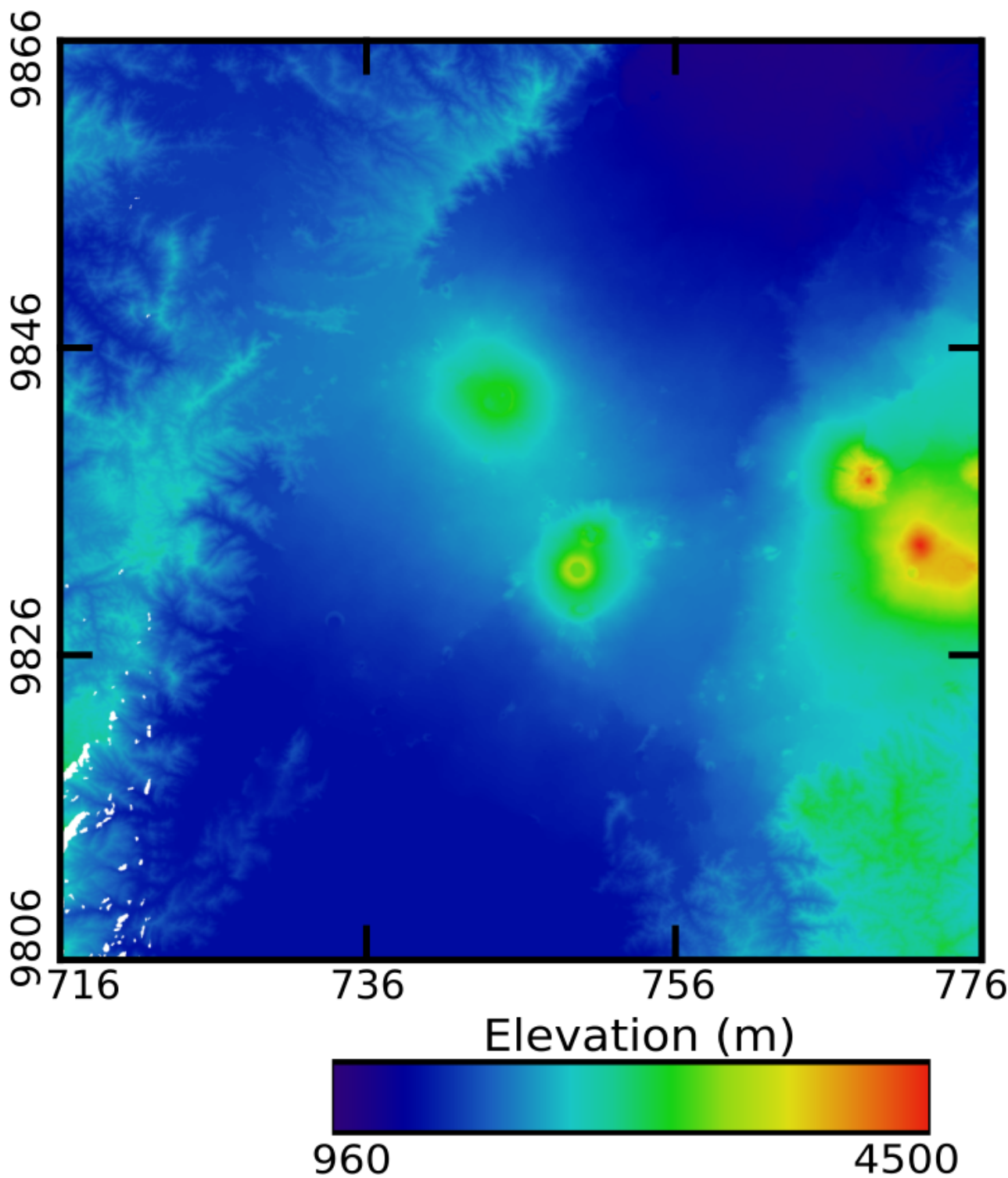


Figure S23. Digital Elevation Model (SRTM 30 m) of VVP.